Oxidation-induced activation of chalcogen bonding in redox-active bis(selenomethyl)tetrathiafulvalene derivatives

Maxime Beau, Olivier Jeannin, Marc Fourmigué, Pascale Auban-Senzier, F Barriere, Ie-Rang Jeon

▶ **To cite this version:**

Maxime Beau, Olivier Jeannin, Marc Fourmigué, Pascale Auban-Senzier, F Barriere, et al.. Oxidation-induced activation of chalcogen bonding in redox-active bis(selenomethyl)tetrathiafulvalene derivatives. CrystEngComm, 2022, 24 (43), pp.7535-7539. 10.1039/d2ce01168a . hal-03828323

HAL Id: hal-03828323
https://hal.science/hal-03828323v1

Submitted on 25 Oct 2022

HAL is a multi-disciplinary open access archive for the deposit and dissemination of scientific research documents, whether they are published or not. The documents may come from teaching and research institutions in France or abroad, or from public or private research centers.

L'archive ouverte pluridisciplinaire **HAL**, est destinée au dépôt et à la diffusion de documents scientifiques de niveau recherche, publiés ou non, émanant des établissements d'enseignement et de recherche français ou étrangers, des laboratoires publics ou privés.

Distributed under a Creative Commons Attribution - NonCommercial 4.0 International License

CrystEngComm

ROYAL SOCIETY OF CHEMISTRY

COMMUNICATION

View Article Online
View Journal

Check for updates

Cite this: DOI: 10.1039/d2ce01168a

Received 25th August 2022,
Accepted 7th October 2022

DOI: 10.1039/d2ce01168a

rsc.li/crystengcomm

Oxidation-induced activation of chalcogen bonding in redox-active bis(selenomethyl) tetrathiafulvalene derivatives†

Maxime Beau,[a] Olivier Jeannin,[a] Marc Fourmigué, *[a] Pascale Auban-Senzier,[b] Frédéric Barrière[a] and Ie-Rang Jeon *[a]

Chalcogen bonding (ChB) interactions are investigated in two new –SeMe substituted tetrathiafulvalene (TTF) derivatives, RTTF(SeMe)$_2$ (R = Me$_2$, SCH$_2$CH$_2$S). Upon oxidation to 1:1 cationic radical salts, Se atoms are engaged in highly linear ChB interactions with bromide anions, demonstrating the efficient σ-hole activation of selenium through redox-active substituents.

The ability to control intermolecular interactions in molecular conductors is crucial owing to the critical role of molecular organization in their dimensionality and physical properties.[1] Earlier efforts in this direction include the functionalization of tetrathiafulvalene (TTF) molecules with hydrogen bonding donor groups such as alcohols, carboxylic acids, phosphonic acids, and amides.[2] In parallel, iodine atoms have been also introduced as a peripheric substituent of TTF, to promote intermolecular halogen bonding (XB) interactions.[2,3] Indeed, the iodine atom develops a charge-depleted area along the prolongation of the C$_{TTF}$–I bond, called σ-hole. This positive electrostatic potential area on the iodine becomes further strengthened upon (partial) oxidation of TTF to establish a strong interaction with Lewis bases.[3–6] It has been shown that in the solid state, this strong and directional XB interaction significantly contributes to the crystal packing of TTF-derivatives. This concept of charge-assisted activation of XB in iodo-TTF derivatives has been further proved in solution studies and in charge transfer compounds.[7,8] Altogether, the introduction of iodine atoms on the TTF moiety to activate XB is now well recognized as a powerful strategy in the field of crystal engineering and materials science, including molecular conductors and molecular sensing.[9]

Besides XB, chalcogen bonding (ChB), which is based on σ-holes developed on a group 16 atom, has attracted interest in recent years.[10] In contrast to a single σ-hole on a halogen atom, a divalent chalcogen atom develops two σ-holes in the prolongation of both C–Ch bonds.[11] Moreover, these two σ-holes can strongly deviate from linearity, which makes the application of ChB in crystal engineering often challenging due to the lack of strong directionality and predictability.[12] In the literature, σ-holes of chalcogen atoms are often enhanced by introducing either neutral or charged electron withdrawing substituents, such as perfluoroaryl, ethynyl, cyano, carborane, triazolium, and imidazolium groups (Scheme 1).[13–18] In parallel, chalcogen-containing heterocycles, such as chalcogenadiazoles, chalcogenazole *N*-oxides, and thiazyl radicals, have shown to form stable motifs to build solid-state self-assemblies.[19] Very recently, the electrochemical oxidation of chalcogenoviologens and a bis(ferrocenyltellurotriazole) has proven to control ChB interactions in solution.[20] To this end, use of redox-active

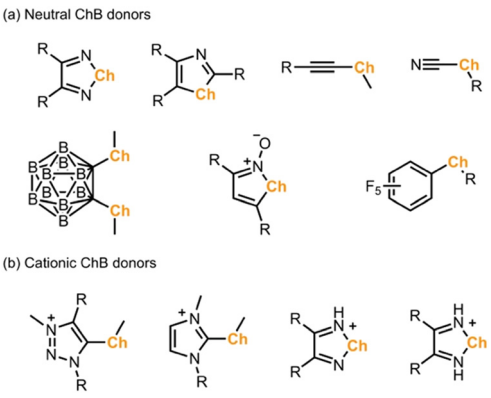

Scheme 1 σ-Hole activating groups in the literature examples of (a) neutral and (b) cationic chalcogen bond (ChB) donors.[13–19]

[a] *Univ Rennes, CNRS, ISCR (Institut des Sciences Chimiques de Rennes), Campus de Beaulieu, 35000 Rennes, France. E-mail: marc.fourmigue@univ-rennes1.fr, ie-rang.jeon@univ-rennes1.fr*

[b] *Laboratoire de Physique des Solides UMR 8502 CNRS-Université Paris-Saclay, Bat 510, 91405 Orsay cedex, France*

† Electronic supplementary information (ESI) available: Experimental details, ESP calculations, crystallographic data, and crystallographic information files (CIF). CCDC 2190022–2190025. For ESI and crystallographic data in CIF or other electronic format see DOI: https://doi.org/10.1039/d2ce01168a

Open Access Article. Published on 10 October 2022. Downloaded on 10/25/2022 10:20:15 AM.
This article is licensed under a Creative Commons Attribution-NonCommercial 3.0 Unported Licence.

Open Access Article. Published on 10 October 2022. Downloaded on 10/25/2022 10:20:15 AM.
This article is licensed under a Creative Commons Attribution-NonCommercial 3.0 Unported Licence.

molecules to activate the ChB *in solid state* has yet to be explored.

Inspired by well-established concept of charge-activation of XB in iodo-TTF derivatives,[3–9] we hypothesized that the installation of chalcogen-containing functional groups on a TTF could be an ideal candidate to demonstrate our idea (Scheme 2). In the literature, Se-containing TTF molecules are often those with an ethylenediseleno group.[21] In this case, the approach of a Lewis base as ChB acceptor might be hindered by the presence of the closed ring to establish an optimized ChB interaction. To this end, we considered, as a proof of concept, to functionalize *ortho*-dimethyl-TTF (*o*-Me_2TTF) and ethylenedithio-TTF (EDT-TTF), with two –SeMe groups to give **1** and **2** (Scheme 2b), in order to release the steric hindrance and to provide a localized interaction site. As a ChB acceptor, bromide anion was chosen due to its negative charge and a spherical shape.

In the literature, symmetric tetrakis(alkylseleno) TTFs have been mostly prepared by lithiation of TTF with LDA followed either by reaction with a dialkyldiselenide or by a selenium insertion and subsequent alkylation.[22] By adapting this procedure, *o*-Me_2TTF (a) was treated with *n*-BuLi followed by an addition of selenium and methylation with CH_3I, to provide *o*-Me_2TTF$(SeMe)_2$ (**1**) in 73% yield (Scheme 3), after recrystallization from EtOAc. For EDT-TTF$(SeMe)_2$, we had to use a different strategy due to the potential reactivity of the ethylene-bridge with *n*-BuLi. Consequently, $P(OEt)_3$ coupling of two different dithiole precursors, namely 4,5-bis(2′-cyanoethylseleno)-1,3-dithiol-2-one (b) and 4,5-ethylenedithio-1,3-dithiol-2-thione (c) at 80 °C afforded 4,5-ethylenedithio-6,7-bis(2′-cyanoethylseleno)TTF (d) in 77% yield.[23] Deprotection of d with $CsOH{\cdot}H_2O$, followed by methylation with CH_3I afforded EDT-TTF$(SeMe)_2$ (**2**) in 87% yield after recrystallization in MeCN.

The neutral donor molecule **1** crystallizes in the monoclinic system, space group $P2_1/c$ with the molecule located in a general position. The TTF core is strongly

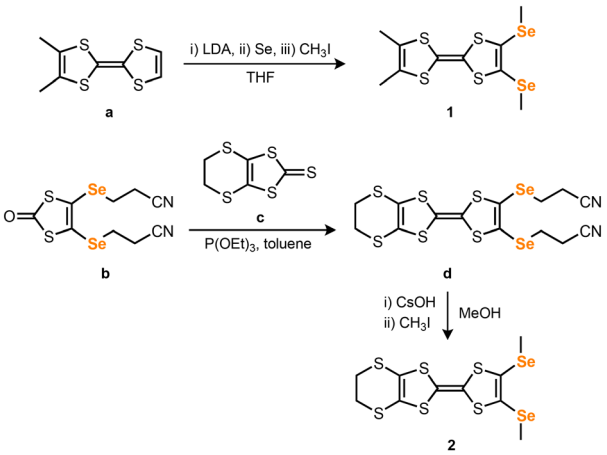

Scheme 3 Synthesis of compounds **1** and **2**.

distorted from planarity. The folding angle along the S1···S2 hinge, defined as a dihedral angle between the mean plane through S1, C1, and S2 and that through S1, C2, C3, and S2, is 25.5(3)°. The analogous one along the S3···S4 hinge is 9.3(3)° (Fig. 1a and b). The methyl group on Se1 is in-plane while the one on Se2 is out-of-plane. Two TTF molecules are dimerized by facing each other in a head-to-tail fashion without a significant orbital overlap, reflecting their neutral closed-shell character.

In the solid state, the dimers are arranged in a sandwich herringbone pattern in the *bc* plane (Fig. S5†). As shown in Fig. 1c, the inversion centre generates Ch···Ch interaction between two Se1 atoms of neighbouring molecules with the C–Se···Se angle of 150.5(2)° and the Se···Se distance of 3.415(3) Å. In addition, Se1 and Se2 interact with *d*(Se1···Se2) = 3.620(2) Å. Overall, the structure in the solid state organizes into layers in the *ac* plane with a segregation of –SeMe moieties through interactions between chalcogen atoms.

The neutral donor molecule **2** crystallizes in the monoclinic system, space group $P2_1/c$ with two molecules in the asymmetric unit (Fig. 2). One molecule is close to planar

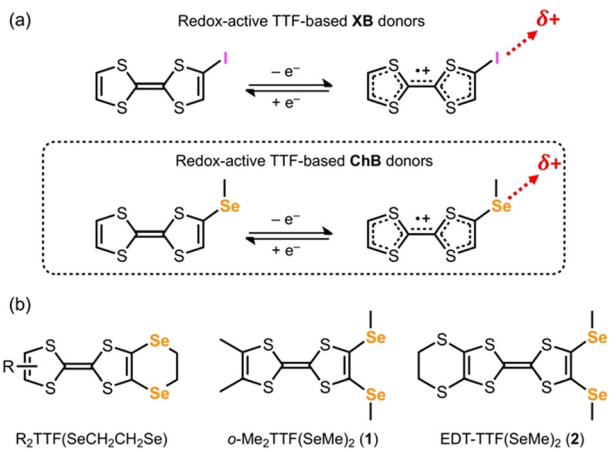

Scheme 2 (a) The concept of charge-assisted σ-hole activation upon oxidation in redox-active TTF-based XB and ChB donors and (b) Se-containing TTFs in the literature[21] and in this work.

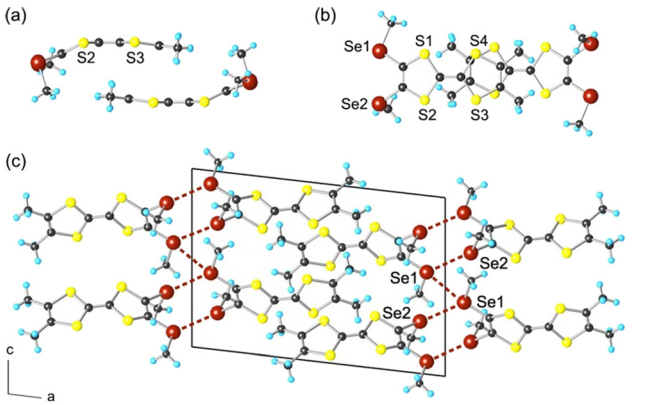

Fig. 1 Structure of neutral **1** with (a) overlap pattern within a dimer; (b) projection view along *a* axis; (c) projection view along *b* axis with details of ChB interactions in dashed lines.

This journal is © The Royal Society of Chemistry 2022

Open Access Article. Published on 10 October 2022. Downloaded on 10/25/2022 10:20:15 AM.
This article is licensed under a Creative Commons Attribution-NonCommercial 3.0 Unported Licence.

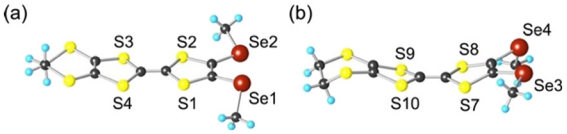

Fig. 2 Two crystallographically independent molecules of neutral **2**, highlighting (a) planar and (b) distorted structures.

with a folding angle of 12.9(4)° along the S3···S4 hinge. The other one is severely distorted from planarity with folding angle of 18.2(4) and 20.0(5)° along the S7···S8 and S9···S10 hinges, respectively. Among four Se atoms within both molecules, Se4 atom is engaged in two short contacts with the S5 and S6 atoms of dithioethylene bridges of two neighbouring molecules (Fig. S6†).

The σ-hole activation on Se atom upon oxidation of TTF units has been first evaluated through the electrostatic potential surfaces (ESP) calculations of the neutral and the oxidized molecules on their optimized geometry. As shown in Fig. 3, a directional σ-hole, represented by an intense blue region, is estimated along the elongation of the C_{TTF}–Se bond. Upon oxidation, the calculated ESP value on Se atoms increases from 19.7 to 85.7 kcal mol^{-1} for **1** and from 21.4 to 84.6 kcal mol^{-1} for **2** (Fig. S8†). The estimated σ-hole on Se atom is found to be as deep as the one on iodine in iodo-TTF,[5b] implying strong activation. Once oxidized, notably the S atoms from the dithiole rings as well as those on the dithioethylene bridge also provide strongly electron deficient regions (*ca.* 75 kcal mol^{-1}, Fig. S9†), which is consistent with what we have previously calculated for the iodinated TTF derivative.[5b] The region of highly positive electrostatic potential on S atoms explains the additional ChB interactions observed in the structure of both radical salts (*vide infra*).

To experimentally investigate the activation of Se σ-hole upon TTF oxidation, electrocrystallizations of **1** and **2** were performed by the galvanostatic oxidation of a MeCN solution in the presence of PPh_4Br and Et_4NBr respectively as electrolytes.

The bromide salt of **1** crystallizes in the monoclinic system, space group $P2_1/n$ with $\mathbf{1}^{+\bullet}$ cation and one bromide in general position, hence the 1 : 1 stoichiometry. The cations are essentially planar and stack along the *a* axis. Within the stack, they are related by an inversion center, forming head-to-tail dyads adopting the bond-over-ring geometry (Fig. S10a†). The intra-dimer and inter-dimer plane-to-plane distances are 3.409 and 3.590 Å, respectively, in a chain of $\mathbf{1}^{+\bullet}$ radical cations (Fig. S10b†). As shown in Table 1, close examination of intramolecular bond distances of $\mathbf{1}^{+\bullet}$ reveals a notable lengthening of the C=C double bond and a shortening of C–S single bonds compared to **1**, confirming its oxidized character. Calculations of the $\beta_{HOMO-HOMO}$ interaction energies for the intra- and inter-dimer overlap interactions give $|\beta|$ values of respectively 0.670 and 0.347 eV, confirming the strong dimerization of the radical species within the chains.

In the solid-state, the σ-hole of both Se1 and Se2 atoms are activated in the prolongation of the C_{TTF}–Se bond, as hypothesized, to interact each with a bromide to make a chain network (Fig. 4). The observed ChB is highly linear (∠C–Se···Br = 176.4(3) – 177.1(3)°) with Se···Br distances (3.367(2)–3.442(2) Å) much shorter than the contact distance (3.72 Å), giving a reduction ratio (RR) down to 0.91. Moreover, S1 and S4 atoms of the dithiole rings of $\mathbf{1}^{+\bullet}$ complete the coordination sites of the bromide through secondary, weaker ChBs, affording a μ_4 geometry of a distorted tetrahedral around the bromide. The S···Br^- distances amount to 3.640(3) (RR 0.97) and 3.835(3) Å (RR 1.01), respectively. It is worth to mention that the apparition of a charge-depleted area between two dithiole rings is predicted in the ESP calculations, with the estimated electrostatic potential to be similarly high as the one on the Se atom (Fig. S9†). Albeit the high charge-depleted character of these S atoms, steric hindrance likely limits ChB interactions, resulting here in higher RR values.

The bromide salt of **2** crystallizes in the monoclinic system, space group $P2_1/c$. The asymmetric unit comprises one $\mathbf{2}^{+\bullet}$ cation and one bromide, hence 1 : 1 stoichiometry. The two SeMe groups are in-plane with the TTF core while the ethylene bridge is distorted out-of-plane (Fig. S12†). As shown in Table 1, intramolecular bond lengths within the donor molecule confirm its oxidized state as a radical cation. The molecules stack into a uniform chain by translation along the *a* axis with an intermolecular distance of 3.56 Å.

As shown in Fig. 5, the bromide anions are engaged in directional ChB interaction with one of two Se atoms

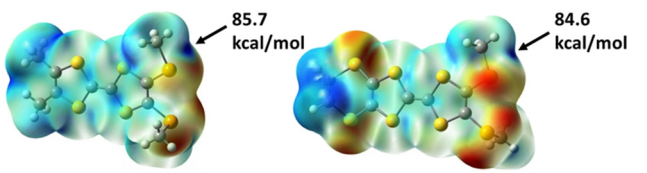

Fig. 3 ESP maps of $\mathbf{1}^{+\bullet}$ (left) and $\mathbf{2}^{+\bullet}$ (right) at 0.001 e bohr^{-3} isosurface with V_S values on Se atoms. Potential scales from +43.9 (red) to +84.7 (blue) kcal mol^{-1}.

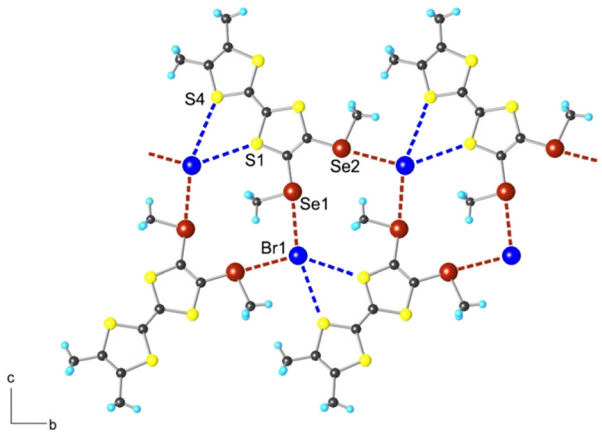

Fig. 4 Structure of **1**(Br) with ChB details.

Open Access Article. Published on 10 October 2022. Downloaded on 10/25/2022 10:20:15 AM.
This article is licensed under a Creative Commons Attribution-NonCommercial 3.0 Unported Licence.

Table 1 Bond distances (Å) in the neutral **1** and **2** compared with the oxidized $\mathbf{1}^{+\bullet}$ and $\mathbf{2}^{+\bullet}$[a]

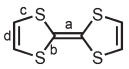

	a	*b*	*c*	*d*
1	1.347(9)	1.754(7)	1.761(7)	1.321(9)
$\mathbf{1}^{+\bullet}$	1.389(10)	1.726(10)	1.732(10)	1.379(10)
2a[b]	1.356(8)	1.755(7)	1.756(6)	1.332(10)
2b[c]	1.340(10)	1.758(6)	1.750(7)	1.342(8)
$\mathbf{2}^{+\bullet}$	1.385(5)	1.726(4)	1.736(4)	1.361(5)

[a] Bond distances were averaged. [b] Molecule with Se1 and Se2. [c] Molecule with Se3 and Se4.

(∠C–Se1···Br = 174.3(1)°). The Se1···Br distance is 3.502(1) Å, yielding RR of 0.92. The bromide anion is also engaged in short S···Br contacts with one S atom from a dithiole ring and another one from the dithioethylene bridge of the same molecule, where a region of positive electrostatic potential was predicted from the ESP calculations (Fig. S9†). The S···Br distances amount to 3.430(3) and 3.449(2) Å for S4···Br1 and S6···Br2 respectively, which corresponds to a RR of 0.95 relative to the contact distance of 3.62 = 1.80 (S) + 1.82 Å (Br^-) Å. These two S···Br^- ChB interactions complement the coordination sphere of the bromide anion, and consequently form a cyclic motif consisting of two TTF molecules and two bromide anions.

Contrary to the structure of strongly dimerized TTFs in (**1**)Br, (**2**)Br adopts a uniform chain structure with a sizeable orbital overlap ($|\beta_{HOMO-HOMO}|$ = 0.303 eV) between $\mathbf{2}^{+\bullet}$ radical cations (Fig. S12†), motivating us to investigate variable-temperature resistivity. The resistivity of this compound shows a semi-conducting behaviour with $\rho \approx 8\ \Omega$ cm at 300 K (Fig. S14†). Fitting the data with an activation law, $\rho = \rho_0 \exp(E_a/T)$, shows an increase of the activation energy E_a upon cooling, from 0.10 eV (1160 K) determined between 300 and 250 K to 0.16 eV (1900 K) determined between 200 and 160 K. The evolution of the activated regime leading to a higher activation energy at lower temperature likely indicates a progressive dimerization of the stack upon cooling.

Altogether, both oxidized radical salts (**1**)Br and (**2**)Br successfully reveal the apparition of highly linear ChB interactions between Se and bromide anions (174.3–177.1°), demonstrating the efficient σ-hole activation upon oxidation.

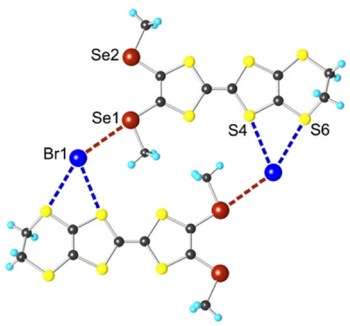

Fig. 5 Structure of **2**(Br) with ChB details.

Moreover, the observed RR (0.91–0.92) is quite significant for a ChB involving a Se atom. It is worth to note that several attempts to obtain co-crystals of neutral **1** and **2** with $(Bu_4N)Br$ and $(PPh_4)Br$, were unsuccessful, which can be in part explained by much weaker interaction between non-activated Se and bromide anion with the neutral **1** and **2** molecules.

In the literature, there exist indeed several 1:1 cationic radical salts of alkylseleno-TTF derivatives, which show short contacts with anions such as I_3^-, ReO_4^-, $[Fe(CN)_6]^{3-}$, $[Au(CN)_2]^-$ and $FeBr_4^-$ (Table S2 and Fig. S15†).[24] In these examples, TTFs are mostly functionalized with ethylenediseleno groups (*Cf* Scheme 2). Consequently, although the observed intermolecular interactions between Se atom and an anion can be short with RR values ranging between 0.87 and 0.99, one can notice that the related angles are mostly not highly linear (135–173°). Given that the efficiency of a nonconvalent interaction and the formation of a synthon are determined by both directionality and strength,[25] the observed C_{TTF}–Se···Br^- angles in (**1**)Br and (**2**)Br are the signature of an efficient interaction.

The foregoing results describe an oxidation-induced activation of ChB in two new TTF derivatives. Impressively, the observed ChBs are highly linear, proving the efficiency of the interaction originated from the well-disposed –SeMe functional groups in contrast to the ethylenediseleno group. In both radical salts, the coordination sphere of the bromide anion is complemented by secondary weaker ChB interactions with S atoms of dithiole rings. Work is underway to further introduce such ChB interactions within charge-transfer salts involving organic electron-acceptors (TCNQ, $TCNQF_4$, …).

Author contributions

I. J. and M. F. conceived the project. M. B. synthesized and crystallized the compounds. O. J. collected and solved X-ray diffraction data. M. F. and F. B. performed the calculations. P. A. performed electric resistivity measurements. I. J. wrote the paper and all the authors contributed to revising it.

Conflicts of interest

There are no conflicts to declare.

 This journal is © The Royal Society of Chemistry 2022

Open Access Article. Published on 10 October 2022. Downloaded on 10/25/2022 10:20:15 AM.
This article is licensed under a Creative Commons Attribution-NonCommercial 3.0 Unported Licence.

Acknowledgements

This research was supported by the French National Research Agency Grant, ANR 17-ERC3-0003 and a PhD grant (to M. Beau) from Région Bretagne. We thank N. Quéméré for his help on the synthesis of **2** and the CDIFX in Rennes for the use of X-ray diffractometer. This work was granted access to the HPC resources of CEA-TGCC under the allocation 2022-AD010805032R1 awarded by GENCI.

Notes and references

1 G. Saito and Y. Yoshida, *Top. Curr. Chem.*, 2012, **312**, 67.
2 M. Fourmigué and P. Batail, *Chem. Rev.*, 2004, **104**, 5379.
3 T. Imakubo, H. Sawa and R. Kato, *Synth. Met.*, 1995, **73**, 117.
4 A. S. Batsanov, M. R. Bryce, A. Chesney, J. A. K. Howard, D. E. John, A. J. Moore, C. L. Wood, H. Gershtenman, J. Y. Becker, V. Y. Khodorkovsky, A. Ellern, J. Bernstein, I. F. Perepichka, V. Rotello, M. Gray and A. O. Cuello, *J. Mater. Chem.*, 2001, **11**, 2181.
5 (*a*) O. Jeannin, E. Canadell, P. Auban-Senzier and M. Fourmigué, *Chem. Commun.*, 2016, **52**, 308; (*b*) M. Beau, O. Jeannin, S. Lee, F. Barrière, M. Fourmigué and I.-R. Jeon, *ChemPlusChem*, 2020, **85**, 2136.
6 (*a*) J. Nishijo, E. Ogura, J. Yamaura, A. Miyazaki, T. Enoki, T. Takano T. Y. Kuwatani and M. Iyoda, *Solid State Commun.*, 2000, **116**, 661; (*b*) T. Devic, B. Domercq, P. Auban-Senzier, P. Molinié and M. Fourmigué, *Eur. J. Inorg. Chem.*, 2002, 2844; (*c*) A. Ranganathan, A. El-Ghayoury, C. Mézière, E. Harté, R. Clérac and P. Batail, *Chem. Commun.*, 2006, 2878.
7 R. Oliveira, S. Groni, C. Fave, M. Branca, F. Mavré, D. Lorcy, M. Fourmigué and B. Schöllhorn, *Phys. Chem. Chem. Phys.*, 2016, **18**, 15867.
8 J. Lieffrig, O. Jeannin, A. Frąckowiak, I. Olejniczak, R. Świetlik, S. Dahaoui, E. Aubert, E. Espinosa, P. Auban-Senzier and M. Fourmigué, *Chem. – Eur. J.*, 2013, **19**, 14804.
9 (*a*) M. Fourmigué, *Struct. Bonding*, 2008, **126**, 181; (*b*) C. Fave and B. Schöllhorn, *Curr. Opin. Electrochem.*, 2019, **15**, 89.
10 P. Scilabra, G. Terraneo and G. Resnati, *Acc. Chem. Res.*, 2019, **52**, 1313.
11 L. Vogel, P. Wonner and S. M. Huber, *Angew. Chem., Int. Ed.*, 2019, **58**, 1880.
12 (*a*) W. Wang, B. Ji and Y. Zhang, *J. Phys. Chem. A*, 2009, **113**, 8132; (*b*) E. Alikhani, F. Fuster, B. Madebene and G. J. Grabowski, *Phys. Chem. Chem. Phys.*, 2014, **16**, 2430; (*c*) D. J. Pascoe, K. B. Lin and S. L. Cockroft, *J. Am. Chem. Soc.*, 2017, **139**, 15160.
13 (*a*) S. Benz, A. I. Poblador-Bahamonde, N. Low-Ders and S. Matile, *Angew. Chem., Int. Ed.*, 2018, **57**, 5408; (*b*) G. E. Garrett, E. I. Carrera, D. S. Seferos and M. S. Taylor, *Chem. Commun.*, 2016, **52**, 9881.
14 A. Dhaka, O. Jeannin, I.-R. Jeon, E. Aubert, E. Espinosa and M. Fourmigué, *Angew. Chem., Int. Ed.*, 2020, **59**, 23583.
15 H.-T. Huynh, O. Jeannin and M. Fourmigué, *Chem. Commun.*, 2017, **53**, 8467.
16 M. Beau, S. Lee, S. Kim, W.-S. Han, O. Jeannin, M. Fourmigué, E. Aubert, E. Espinosa and I.-R. Jeon, *Angew. Chem., Int. Ed.*, 2021, **60**, 366.
17 J. Y. C. Lim, I. Marques, A. L. Thompson, K. E. Christensen, V. Félix and P. D. Beer, *J. Am. Chem. Soc.*, 2017, **139**, 3122.
18 (*a*) P. Wonner, L. Vogel, M. Düser, L. Gomes, F. Kniep, B. Mallick, D. B. Werz and S. M. Huber, *Angew. Chem., Int. Ed.*, 2017, **56**, 12009; (*b*) L. M. Lee, V. B. Corless, M. Tran, H. Jenkins, J. F. Britten and I. Vargas-Baca, *Dalton Trans.*, 2016, **45**, 3285.
19 (*a*) A. F. Cozzolino, P. J. W. Elder and I. Vargas-Baca, *Coord. Chem. Rev.*, 2011, **255**, 1426; (*b*) L.-J. Riwar, N. Trapp, K. Root, R. Zenobi and F. Diederich, *Angew. Chem., Int. Ed.*, 2018, **57**, 17259; (*c*) A. Kremer, A. Fermi, N. Biot, J. Wouters and D. Bonifazi, *Chem. – Eur. J.*, 2016, **22**, 5665; (*d*) M. B. Mills, H. K. S. Young, G. Wehrle, W. R. Verduyn, X. Feng, P. D. Boyle, P. Dechambenoit, E. R. Johnson and K. E. Preuss, *Cryst. Growth Des.*, 2021, **21**, 5669; (*e*) M. Risto, A. Assoud, S. M. Winter, R. Oilunkaniemi, R. S. Laitinen and R. T. Oakley, *Inorg. Chem.*, 2008, **47**, 10100; (*f*) T. M. Barclay, A. W. Cordes, J. D. Goddard, R. C. Mawhinney, R. T. Oakley, K. E. Preuss and R. W. Reed, *J. Am. Chem. Soc.*, 1997, **119**, 12136.
20 R. Hein, A. Docker, J. J. Davis and P. D. Beer, *J. Am. Chem. Soc.*, 2022, **144**, 8827.
21 (*a*) M. Clemente-Leon, E. Coronado, J. R. Galan-Mascaros, C. Gimenez-Saiz, C. J. Gomez-Garcia, J. M. Fabre, G. A. Mousdis and G. C. Papavassiliou, *J. Solid State Chem.*, 2002, **168**, 616; (*b*) K. Furuta, S. Kohno, T. Shirahata and Y. Misaki, *Eur. J. Inorg. Chem.*, 2014, **2014**, 3982; (*c*) M. Enomoto, A. Miyazaki and T. Enoki, *Bull. Chem. Soc. Jpn.*, 2001, **74**, 459.
22 (*a*) A. J. Moore, M. R. Bryce, G. Cooke, G. J. Marshallsay, P. J. Skabara, A. S. Batsanov, J. A. K. Howard and S. T. A. K. Daley, *J. Chem. Soc., Perkin Trans. 1*, 1993, **1**, 1403; (*b*) A. M. Kini, B. D. Gates, G. A. Beno and J. M. Williams, *J. Chem. Soc., Chem. Commun.*, 1989, 169; (*c*) S.-Y. Hsu and L. Y. Chiang, *J. Org. Chem.*, 1987, **52**, 3445.
23 L. Boudiba, L. Kaboub, A. Gouasmia and J. M. Fabre, *Synthesis*, 2005, **8**, 1291.
24 (*a*) M. Clement-Leon, E. Coronado, J. R. Galan-Mascaros, C. Gimenez-Saiz, C. J. Gomez-Garcia, J. M. Fabre, G. A. Mousdis and G. C. Papavassiliou, *J. Solid State Chem.*, 2002, **168**, 616; (*b*) P. Wang, T. Inabe, C. Nakano, Y. Maruyama, H. Inokuchi, N. Iwasawa and G. Saito, *Bull. Chem. Soc. Jpn.*, 1989, **62**, 2252; (*c*) M. Enomoto, A. Miyazaki and T. Enoki, *Bull. Chem. Soc. Jpn.*, 2001, **74**, 459; (*d*) K. Furuta, S. Kohno, T. Shirahata, K. Yamasaki, S. Hino and Y. Misaki, *Crystals*, 2012, **2**, 393.
25 T. Steiner, *New J. Chem.*, 1998, 1099; M. E. Brezgunova, E. Aubert, S. Dahaoui, P. Fertey, S. Lebègue, C. Jelsch, J. G. Ángyán and E. Espinosa, *Cryst. Growth Des.*, 2012, **12**, 5373.